Aalborg Universitet

AALBORG UNIVERSITY
DENMARK

Modeling Thermal Conductivity of Highly Filled Polymer Composites

Drozdov, Aleksey D.; Christiansen, Jesper de Claville

Modeling thermal conductivity of highly filled polymer composites

A.D. Drozdov and J. deClaville Christiansen

Department of Materials and Production

Aalborg University

Fibigerstraede 16, Aalborg 9220, Denmark

Abstract

The Kanari model is traditionally treated as an empirical relation to fit observations on the effective thermal conductivity of composites. By applying the integration embedding method, we demonstrate that this model provides an extension of the Halpin–Tsai and Fricke models to highly filled composites, and the only adjustable parameter in the governing equation is expressed in terms of the aspect ratio of filler particles and their aggregates. These assertions are confirmed by the analysis of observations on several polymer composites.

Key-words: Polymer composite; Thermal conductivity; Integration embedding method; Thermal interface material

Introduction

Thermal conductivity of polymer composites highly filled with ceramic, metal and carbon particles has recently attracted substantial attention [1, 2, 3]. This interest may be explained by excellent properties of composites with polymeric matrices (light weight, low cost, ease of processing, low processing temperatures, stability under a humid environment), as well as by a number of their ap- plications in industry. Polymer-ceramic composites are widely used as thermal interface materials in packaging of a new generation

of electronic equipments (light-emitting devices and integrated cir- cuits) and ultrahigh-voltage electrical devices [4, 5]. Polymer-metal and polymer-carbon composites with high dielectric constants are applied as materials for shielding of electromagnetic interference [6, 7] and radar absorbing systems [8, 9].

Most polymers posess rather low thermal conductivity randing from 0.1 to 0.5 W/(m·K). To develop thermal interface materials for electronic packaging with conductivities in the interval from 5 to 10 W/(m·K), they should be incorporated with large volume fractions (above 50%) of highly conducting inorganic fillers (boron nitride, silicon carbide, silicon nitride, etc.), whose thermal conductivities exceed those of the matrices by two to three orders of magnitude. Since processing of highly filled composites is difficult, a number of strategies have recently been designed to reduce volume fractions of filler [10]. They involve (i) chemical functionalization of matrices and fillers [11], (ii) development of novel routes of preparation of composites [12], (iii) alignment of particles with high aspect ratios [13], (iv) reinforcement of polymers with hybrid fillers [14], (v) formation of hierarchically ordered interconnected networks of particles [15], (vi) manufacturing composites with segregated fillers [16], and (vii) combination of the above methods [17].

To compare different approaches to manufacturing thermally conductive composites and to evaluate their efficacies, it seems natural to apply mathematical modeling. During the past century, a number of models have been developed for thermal conductivity of composites, see recent reviews [18, 19, 20]. Following [21], these models can be split into two groups: (i) theoretical models with transparent physical meaning of their coefficients, and (ii) empirical models with no correlation between the parameters found by fitting experimental data and the micro-structure of composites. Analysis of observations on highly filled polymer composites with large ratios of thermal conductivities of the filler and matrix shows that conventional theoretical models underestimate the effective thermal conductivity. This is not surprising as there models are based on the mean field approximation, which disregards interactions between filler particles. In highly filled composites, these interactions play the key role in thermal conductivity due to aggregation of filler into clusters and formation of conductive paths along the filler particles and their

2

aggregates.

The present work focuses on the study of the Kanari model [22], which was initially introduced as an "empirical" relation for the description of thermal conductivity of highly filled composites.

Our objective is to demonstrate that (i) this model is "theoretical" in the sense of [21], which means that it can be derived from the conventional mean-field concepts (the Halpin–Tsai and the Fricke models) by the integration embedding scheme, (ii) the only adjustable constant in the Kanari model has a transparent physical meaning (it is expressed in terms of the aspect ratio of filler particles and their aggregates), and (iii) the quality of matching observations by means of the Kanari model is superior compared with other empirical models (the Nielsen and the Agari models) involving two adjustable parameters.

Models for thermal conductivity

We start with a brief discussion of governing equations for the effective thermal conductivity of composites with relatively small volume fractions of filler ϕ (when conditions for the dilute suspension approximation are satisfied). The matrix of a composite is presumed to be an isotropic and homogeneous medium with thermal conductivity k_m. Filler particles are treated as isotropic and homogeneous materials with thermal conductivity k_f. These particles are presumed to be randomly distributed in the matrix. To take into account the thermal contact resistance at the interface be- tween the matrix and the filler, the thermal conductivity k_f should be replaced with its effective value k_f^*. For spherical inclusions with radius a, the coefficient k_f^* is found from the equation [23]

$$\frac{k_f^*}{k_m} = \left(1 + \frac{k_f^*}{k_m}\frac{a_K}{a}\right)^{-1} \tag{1}$$

where a_K stands for the Kapitza radius. Similar relations for the effective thermal conductivity of non-spherical particles and of spherical particles with a generalized law of

3

thermal resistance are reported in [24] and [25]. To simplify the notation, we omit the asterisk in what follows and treat k_f as the effective thermal conductivity of filler.

When all filler particles are spherical and interactions between them are neglected, the effective thermal conductivity of a composite k_c is determined as a solution of the Maxwell equation

$$\frac{X-1}{X+2} = \phi\frac{R-1}{R+2} \qquad (2)$$

where

$$X = \frac{k_c}{k_m}, \qquad R = \frac{k_f}{k_m} \qquad (3)$$

Resolving Eqs. (2) and (3) with respect to k_c, we arrive at the Maxwell formula

$$\frac{k_c}{k_m} = \frac{3\phi(k_f - k_m)}{k_f + 2k_m - \phi(k_f - k_m)} . \qquad (4)$$

When shape of filler particles does not differ substantially from spherical, the thermal conductivity of a composite is determined by the Halpin–Tsai equation [26, 27]

$$\frac{k_c}{k_m} = \frac{1 + a\,\beta\,\phi}{1 - \beta\phi} \qquad (5)$$

with

$$\beta = \frac{R-1}{R+a}, \qquad a = A - 1, \qquad (6)$$

4

where A is an adjustable parameter, the so-called Einstein coefficient [27].

For composites with spheroidal inclusions (ellipsoids of rotation with semi-axes a_1 and $a_2 = a_3$), the effective thermal conductivity is given by the Fricke relation [28]

$$\frac{X - 1}{X + b} = \Phi \frac{R - 1}{R + b} \tag{7}$$

which coincides with Eq. (2) for $b = 2$. It follows from Eq. (7) that

$$\frac{k_c}{k_m} = 1 + \frac{B \, \Phi \, (k_f - k_m)}{k_f - (B - 1)k_m - \Phi(k_f - k_m)} \tag{8}$$

where $B = b + 1$. The coefficient B reads

$$B = \frac{\alpha(R - 1)}{(R - 1) - \alpha} \tag{9}$$

where

$$\alpha = \frac{R - 1}{3} \left[\frac{2}{1 + \dfrac{L(R - 1)}{2}} + \frac{1}{1 + (1 - L)(R - 1)} \right] \tag{10}$$

and L is expressed in terms of the ratio $\frac{a_1}{a_2}$.

When the thermal conductivity of filler exceeds strongly that of the matrix ($R \gg 1$), Eqs. (9) and (10) imply that

$$B = \frac{4 - 3L}{3L(1 - L)} \tag{11}$$

where

$$L = \frac{1}{\sin^2\phi} - \frac{\cos^2\phi}{2\sin^3\phi}\ln\left(\frac{1+\sin\phi}{1-\sin\phi}\right), \qquad \cos\phi = \frac{a_2}{a_1} \quad (a_1 > a_2)$$

$$L = \frac{2\phi - \sin 2\phi}{2\sin^2\phi}\cos\phi, \quad \cos\phi = \frac{a_1}{a_2} \qquad (a_1 < a_2). \tag{12}$$

Up to notation, Eqs. (12) coincide with the corresponding formulas reported in [29]. For spherical particles with $a_1 = a_2$, Eqs. (11) and (12) imply that

$$L = \frac{2}{3}, \quad B = 3,$$

and Eq. (8) is transformed into Eq. (4). For arbitrary parameters a_1 and a_2, the effect of their ratio on the coefficient B is illustrated in Fig. 1.

Eqs. (4), (5) and (8) describe adequately an increase in thermal conductivity of composites k_c with ϕ at volume fractions of filler below 0.1 to 0.2, but fail to predict experimental data at larger concentrations, when interactions between filler particles become noticeable.

Thermal conductivity of a composite with interacting spherical particles is described by means of the Bruggeman model [30], where k_c is determined as a solution of the nonlinear equation

$$\frac{k_f - k_c}{k_f - k_m}\left(\frac{k_m}{k_c}\right)^{\frac{1}{3}} = 1 - \phi. \tag{13}$$

Eq. (13) can be derived from the Maxwell equation (4) by means of the integration embedding scheme [31]. To the best of our knowledge, no analogs of Eq. (13) have been developed for non- spherical filler particles. It is worth mentioning, however, the work [32], where the Bruggerman method was employed to evaluate the influence of interfacial thermal resistance on thermal conductivity of composites with spherical particles, and

[33], where a similar approach was applied to the analysis of thermal conductivity of multiphase composites with spherical inclusions.

The effective thermal conductivity of composites highly filled with spheroidal particles is con- ventionally determined by means of the Mori-Tanaka micromechanical models [34, 35] or with the help of empirical expressions. Although the micromechanical approach is based on a solid theoretical ground, it requires rather complicated simulation (explicit formulas are developed for spherical inclusions only), while results of numerical analysis do not differ noticeably from those determined by means of empirical models [36].

The following three empirical models are used to fit observations.

To account for aggregation of filler particles, Nielsen [27] proposed to include an extra function Ψ in Eq. (5),

$$\frac{k_c}{k_m} = \frac{1 + a\,\beta\phi}{1 - \beta\Psi\,\phi}\,, \qquad \Psi = 1 + \frac{1 - \phi_{max}}{\phi_{max}^2} \qquad (14)$$

where the maximum packing fraction of filler ϕ_{max} was treated as an adjustable parameter. The presence of the function Ψ in the denominator in Eq. (14) ensures a pronounced growth of k_c when ϕ approaches ϕ_{max} .

Kanari [22] suggested to replace the exponent $^1/_3$ in Eq. (13) with the fraction $^1/_M$ to obtain

$$\frac{k_f - k_m}{k_f - k_m}(\frac{k_m}{k_c})^{\frac{1}{M}} = 1 - \phi \qquad (15)$$

with M treated as an adjustable parameter. Although good agreement between experimental data and results of simulation based on Eq. (15) has been demonstrated by several authors, the applicability of Eq. (15) remains limited due to an unclear physical

meaning of the exponent M.

Agari [37, 38] argued that a pronounced growth of the thermal conductivity of a composite k_c with volume fraction of filler ϕ is induced by formation of conductive paths between filler particles and their aggregates. This phenomenon is described by the empirical equation

$$\log k_c = (1 - \phi) \log(C_1 k_m) + C_2 \phi \log k_f ,\tag{16}$$

where $\log = \log_{10}$, and C_1, C_2 are dimensionless parameters of order of unity (when k_c, k_m and k_f are measured in W/(m·K)). The coefficient C_1 characterizes properties of the matrix, and the coefficient C_2 accounts for the ability of filler particles to form conducting paths.

The integration embedding method

According to the integration embedding method, we start with thermal conductivity of a pure matrix (with thermal conductivity k_m) where a small volume of material is replaced with filler (with thermal conductivity k_f). By using one of the formulas (4), (5) or (8), the thermal conductivity of the composite k_c is determined. Afterwards, a new matrix is considered with thermal conductivity k_c, where another small volume of material is replaced with filler, and its thermal conductivity is calculated by using the same approach. In this process, the thermal conductivity of the composite grows from k_m to its final value k_c corresponding to a given volume fraction of filler ϕ.

First, this scheme is illustrated for the Halpin-Tsai equations (5), (6), which is convenient to present in the form

$$\frac{k_c}{k_m} = 1 + \frac{(a + 1)(k_f - k_m)\phi}{k_f + ak_m - (k_f - k_m)\phi}\tag{17}$$

Starting from the pure matrix, in which a small volume $\Delta v = \Delta\phi$ of the matrix material is replaced with filler particles and disregarding terms of higher order of smallness compared with Δv , we find from Eq. (17) that

$$\Delta k = \frac{(a + 1)(k_f - k_m)k_m}{k_f + a\,k_m}\,\Delta v \tag{18}$$

where $\Delta k = k_c - k_m$. To proceed with the algorithm, we (i) to replace k_m in the right-hand side of Eq. (18) with its current value k and (ii) replace Δv with the corresponding increment of the volume fraction $\Delta\phi/(1 - \phi)$. This results in the formula

$$\Delta k = \frac{(a + 1)(k_f - k)k}{k_f + a\,k}\frac{\Delta\phi}{1 - \phi}$$

which is convenient to re-write by replacing the increments with the differentials

$$\frac{k_f + a\,k}{(k_f - k)k}\,dk = (a + 1)\frac{d\phi}{1 - \phi} \tag{19}$$

Eq. (19) is equivalent to the relation

$$\frac{dk}{k} + A\,\frac{dk}{k_f - k} = A\,\frac{d\phi}{1 - \phi} \tag{20}$$

9

where notation (6) is used. Integration of Eq. (20) over k from k_m to k_c and over ϕ from zero to ϕ results in the formula

$$\ln\frac{k_m}{k_c} + A\ln\frac{k_f - k_c}{k_f - k_m} = A\ln(1 - \phi),$$

which implies that

$$\frac{k_f - k_c}{k_f - k_m}\left(\frac{k_m}{k_c}\right)^{\frac{1}{A}} = 1 - \phi. \tag{21}$$

Eq. (21) provides an extension of the Halpin–Tsai model (5), (6) to particulate composites with high volume fractions of filler.

We now consider the Fricke equation (8). When a small volume $\Delta v = \Delta\phi$ of a pure matrix is replaced with filler particles, Eq. (8) implies that the increment of thermal conductivity Δk is given by

$$\Delta k = \frac{B(k_f - k_m)k_m}{k_f + (B - 1)k_m}\Delta v \tag{22}$$

Bearing in mind the similarity between Eqs. (18) and (22), we omit the above calculations and write the final result

$$\frac{k_f - k_c}{k_f - k_m}\left(\frac{k_m}{k_c}\right)^{\frac{1}{B}} = 1 - \phi. \tag{23}$$

which provides an extension of the Fricke model (8) to highly filled composites with spheroidal particles.

Comparison of Eqs. (21) and (23) with Eq. (15) implies that the Kanari equation is not empirical, but it can be deduced from the Halpin–Tsai and Fricke models by means of the integration embedding scheme. The parameter M is the Kanari equation coincides with the

Einstein coefficient A in the Nielsen model and the measure of non-sphericity of particles B in the Fricke model.

Comparison with observations

Our aim now is threefold: (i) to demonstrate the ability of Eq. (23) to match experimental data, (ii) to show that the accuracy of fitting observations by this relation is not worse than that for the Nielsen model (14) and the Agari model (16) conventionally used to describe the effective thermal conductivity, and (iii) to reveal that the coefficient B found in the approximation procedure is close to that predicted by Eqs. (11) and (12).

To solve Eq. (23) numerically, we use notation (3) and re-write it in the form

$$f(X) = 0 \qquad\qquad (24)$$

with

$$f(X) = X^{\frac{1}{B}} - \frac{1}{1-\phi}\frac{R-X}{R-1}$$

The solution of Eq. (24) is found by means of the iterative Newton–Raphson algorithm

$$X_{n+1} = X_n - \frac{f(X_n)}{f'(X_n)}$$

with $X_1 = 1$ and

$$f'(X) = \frac{X^{\frac{1-B}{B}}}{B} + \frac{1}{(R-1)(1-\phi)}.$$

We begin with the analysis of observations [39] on composites with polystyrene and polyethylene matrices reinforced with magnesium oxide particles. This set of data is chosen because it was used by Nielsen [27] to demonstrate capabilities of Eq. (14). The

experimental data together with results of simulation are presented in Fig. 2, where the relative thermal conductivity k_c/k_m is plotted versus volume fraction of filler ϕ. The numerical analysis is performed with parameters k_m and k_f given in [39]. The only adjustable parameter B is found by matching observations on the composite with the polystyrene matrix and used without changes for the composite with the polyethylene matrix (according to Eqs. (11), (12), B is independent of the properties of matrix).

We proceed with matching experimental data [37] on composites with polyethylene matrices reinforced with copper, graphite and alumina particles. This set of data is chosen because it was employed by Agari [37] to show the advantages of Eq. (16). The observations and the results of simulation are reported in Fig. 3. Calculations are conducted with the coefficients k_m and k_f provided in [37]. Each set of data in Fig. 3 is fitted separately with the only parameter B.

Finally, experimental data are approximated on composites for which observations on thermal conductivity are reported together with SEM or TEM images of filler particles and their aggregates. This allows the coefficient B found by matching the experimental dependencies $k_c(\phi)$ to be compared with that calculated by means of Eqs. (11) and (12). First, observations [40] are approximated on composites with epoxy matrices reinforced with silica-coated aluminum nitride, alumina and silica particles. The experimental data and results of numerical analysis are depicted in Fig. 4. Simulation is performed with the parameters k_m and k_f reported in [40]. Each set of observations is matched separately by means of the only parameter B. Fig. 4 shows that the best-fit values of B increase from 3.0 for spherical silica particles (Fig. 1 in [40]) to 3.2 for slightly non-spherical alumina particles (Fig. 2 in [40] demonstrates that the ratio a_2/a_1 varies from 0.7 to 1) to 3.75 for non-spherical AlN particles (according to Fig. 3 in [40], the ratio a_2/a_1 is close to 0.5). Taking the above values of a_2/a_1 as estimates, we calculate B from Fig. 1 and find $B = 3.0$, 3.1 and 3.5, in reasonable agreement with the results presented in Fig. 4.

It is worth noting that for all composites under investigation, the effective thermal conductivity of inclusions k_f^* coincides with their thermal conductivity k_f, which means that a_K in Eq. (1) is negligible compared with a, and the thermal resistance at the interface

can be disregarded.

We now match experimental data [41] on composites with natural rubber matrices reinforced with two types of carbon black: N539 and acetylene black (AB). The data are reported in Fig. 5 together with results of simulation. Thermal conductivity of the matrix $k_m = 0.2$ W/(m·K) was measured in [41]. In the numerical analysis, the values $k_f = 1.6$ W/(m·K), $B = 3.2$ and $k_f = 8.2$ W/(m·K), $B = 4.8$ are used for N539 and AB, respectively. TEM images of filler presented in Fig. 2 of [41] demonstrate that the ratios a_2/a_1 can be estimated as 0.75 for clusters of N539 and 0.3 for aggregates of AB particles. According to Fig. 1, these ratios correspond to $B = 3.1$ (N539) and $B = 5.2$ (AB), in agreement with the results depicted in Fig. 5.

Concluding remarks

By means of the integration embedding scheme, it has been demonstrated that the Kanari model provides an extension of the Halpin–Tsai and Fricke models to highly filled composites (which confirms that it has a strong physical background). It is proved that the exponent M in Eq. (15) coincides with the Einstein coefficient A in the Halpin–Tsai and Nielsen models and the coefficient B in the Fricke model. For composites with large ratios R of the thermal conductivities of filler and matrix, the latter parameter is expressed in terms of the aspect ratio of filler particles and their clusters with the help of Eqs. (11) and (12). The ability of the model to describe experimental data is validated by comparison of results of simulation with observations on several polymer-ceramic composites. It is shown that the adjustable parameter B in Eq. (23) found by matching observations on the effective thermal conductivity is in agreement with that determined from Eqs. and (12) by using SEM and TEM images of filler particles in the composites.

Acknowledgment

References

[1] H. Chen, V.V. Ginzburg, J., Yang, Y. Yang, W. Liu, Y. Huang, L. Du, and B. Chen, *Prog. Polym. Sci.*, **59**, 41 (2016).

[2] N. Burger, A. Laachachi, M. Ferriol, M. Lutz, V. Toniazzo, and D. Ruch, *Prog. Polym. Sci.*, **61**, 1 (2016).

[3] C. Huang, X. Qian, and R. Yang, *Mater. Sci. Eng. R*, **132**, 1 (2018).

[4] A.L. Moore and L. Shi, *Mater. Today*, **17**, 163 (2014).

[5] H.S. Kim, J. Jang, H. Lee, S.Y. Kim, S.H. Kim, J. Kim, Y.C. Jung, and B.J. Yang, *Adv. Eng. Mater.*, **20**, 1800204 (2018).

[6] S. Sankaran, K. Deshmukh, M. Basheer Ahamed, and S.K. Khadheer Pasha, *Composites A*, **114**, 49 (2018).

[7] H. Abbasi, M. Antunes, and J.I. Velasco, *Prog. Mater. Sci.*, **103**, 319 (2019).

[8] R.P. Magisetty, A. Shukla, and B. Kandasubramanian, *J. Electron. Mater.how* , **47**, 6335 (2018).

[9] C.G. Jayalakshmi, A. Inamdar, A. Anand, and B. Kandasubramanian, *J. Appl. Polym. Sci.*, **36**, 47241 (2019).

[10] X. Xu, J. Chen, J. Zhou, and B. Li, *Adv. Mater.*, **30**, 1705544 (2018).

[11] G.H. Kim, D. Lee, A. Shanker, L. Shao, M.S. Kwon, D. Gidley, J. Kim, and K.P. Pipe, *Nat. Mater.*, **14**, 295 (2015).

[12] Y. Hu, G. Du, and N. Chen, *Compos. Sci. Technol.*, **124**, 36 (2016).

[13] C. Yuan, B. Duan, L. Li, B. Xie, M. Huang, and X. Luo, *ACS Appl. Mater. Interfaces*, **7**, 13000 (2015).

[14] C. Chen, Y. Xue, X. Li, Y. Wen, J. Liu, Z. Xue, D. Shi, X. Zhou, X. Xie, and Y.-W. Mai, *Composites A*, **118**, 67 (2019).

[15] J. Hu, Y. Huang, Y. Yao, G. Pan, J. Sun, X. Zeng, R. Sun, J.-B. Xu, B. Song, and C.-P. Wong, *ACS Appl. Mater. Interfaces*, **9**, 13544 (2017).

[16] K. Wu, C. Lei, R. Huang, W. Yang, S. Chai, C. Geng, F. Chen, and Q. Fu, *ACS Appl. Mater. Interfaces*, **9**, 7637 (2017).

[17] Z.-G. Wang, F. Gong, W.-C. Yu, Y.-F. Huang, L. Zhu, J. Lei, J.-Z. Xu, and Z.-M. Li, *Compos. Sci. Technol.*, **162**, 7 (2018).

[18] K. Pietrak and T.S. Wisniewski, *J. Power Technol.*, **95**, 14 (2015).

[19] X. Yang, C. Liang, T. Ma, Y. Guo, J. Kong, J. Gu, M. Chen, and J. Zhu, *Adv. Compos. Hybrid Mater.*, **1**, 207 (2018).

[20] S. Zhai, P. Zhang, Y. Xian, J. Zeng, and B. Shi, *Int. J. Heat Mass Trans.*, **117**, 358 (2018).

[21] R.C. Progelhof, J.L. Thronem, and R.R. Ruetsch, *Polym. Eng. Sci.*, **16**, 615 (1976).

[22] K. Kanari, *Kobunshi*, **26**, 557 (1977).

[23] D.P.H. Hasselman and L.F. Johnson, *J. Compos. Mater.*, **21**, 508 (1987).

[24] C.-W. Nan, G. Liu, Y. Lin, and M. Li, *Appl. Phys. Lett.*, **85**, 3549 (2004).

[25] S.-T. Gu, A.-L. Wang, Y. Xu, and Q.-C. He, *Int. J. Heat Mass Trans.*, **83**, 317 (2015).

[26] J.C. Halpin and J.L. Kardos, *Polym. Eng. Sci.*, **16**, 344 (1976).

[27] L.E. Nielsen, *J. Appl. Polym. Sci.*, **17**, 3819 (1973).

[28] H. Fricke, *Phys. Rev.*, **24**, 575 (1924).

[29] C.-W. Nan, R. Birringer, D.R. Clarke, and H. Gleiter, *J. Appl. Phys.*, **81**, 6692 (1997).

[30] D.A.G. Bruggeman, *Ann. Phys.*, **24**, 636 (1935).

[31] C.-W. Nan, *Prog. Mater. Sci.*, **37**, 1 (1993).

[32] A.G. Every, Y. Tzou, D.P.H. Hasselman, and R. Raj, *Acta Metall. Mater.*, **40**, 123 (1992).

[33] A.N. Norris, *J. Appl. Mech.*, **56**, 83 (1989).

[34] H. Le Quang, *Int. J. Heat Mass Trans.*, **95**, 162 (2016).

[35] N. Bonfoh, C. Dreistadt, and H. Sabar, *Int. J. Heat Mass Trans.*, **108**, 1727 (2017).

[36] W. Tian, L. Qi, X. Chao, J. Liang, and M.W. Fu, *Int. J. Heat Mass Trans.*, **134**, 735 (2019).

[37] Y. Agari and T. Uno, *J. Appl. Polym. Sci.*, **32**, 5705 (1986).

[38] Y. Agari, A. Ueda, M. Tanaka, and S. Nagai, *J. Appl. Polym. Sci.*, **40**, 929 (1990).

[39] D.W. Sundstrom and Y.-D. Lee, *J. Appl. Polym. Sci.*, **16**, 3159 (1972).

[40] C.P. Wong and R.S. Bollampally. *J. Appl. Polym. Sci.*, **74**, 3396 (1999).

[41] J.-P. Song, K.-Y. Tian, L.-X. Ma, W. Li, and S.-C. Yao, *Int. J. Heat Mass Trans.*, **137**, 184 (2019).

Figure legends

Figure 1: Coefficient B versus the ratio of semi-axes for prolate and oblate spheroidal particles.

Figure 2: The relative thermal conductivity k_c/k_m versus volume fraction of filler ϕ. Symbols: experimental data [39] on composites with polystyrene ($\circ - PS$) and polyethylene ($\cdot - PE$) matrices reinforced with MgO particles. Solid lines: results of simulation with Eq. (23) with $k_m = 0.155$ (PS), $k_m = 0.335$ (PE), $B = 3.15$ and $k_f = 54.8$ W/(m·K).

Figure 3: The relative thermal conductivity k_c/k_m versus volume fraction of filler ϕ. Symbols: experimental data [37] on composites with polyethylene matrices reinforced with copper ($\circ$), graphite ($\cdot$) and alumina ($*$) particles. Solid lines: results of simulation with Eq. (23) with $k_m = 0.29$ W/(m·K) and $B = 5.6$, $k_f = 395.8$ ($\circ$), $B = 4.5$, $k_f = 209.2$ ($\cdot$), $B = 3.0$, $k_f = 33.1$ ($*$) W/(m·K).

Figure 4: The relative thermal conductivity k_c/k_m versus volume fraction of filler ϕ. Symbols: experimental data [40] on composites with epoxy matrices reinforced with silica-coated aluminum nitride ($\circ$), alumina ($\cdot$) and silica ($*$) particles. Solid lines: results of simulation with with Eq. (23) $k_m = 0.17$ W/(m·K) and $B = 3.75$, $k_f = 220$ ($\circ$), $B = 3.2$, $k_f = 36$ ($\cdot$), $B = 3.0$, $k_f = 1.6$ ($*$) W/(m·K).

Figure 5: The relative thermal conductivity k_c/k_m versus volume fraction of filler ϕ. Symbols: experimental data [41] on composites with natural-rubber matrices reinforced with acetylene black ($\circ$) and carbon black N539 ($\cdot$) particles. Solid lines: results of simulation with Eq. (23) with $k_m = 0.215$ W/(m·K) and $B = 4.8$, $k_f = 8.2$ ($\circ$), $B = 3.2$, $k_f = 1.6$ ($\cdot$) W/(m·K).
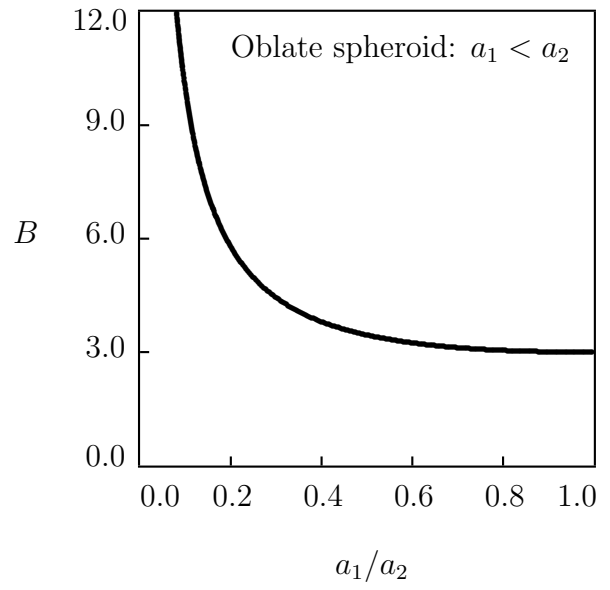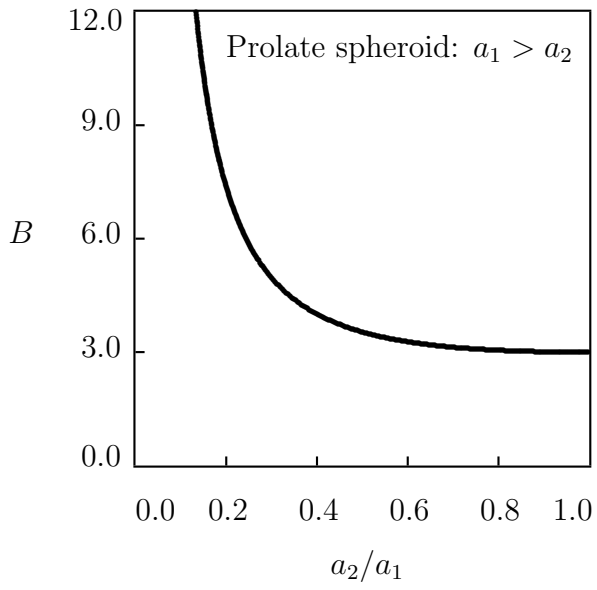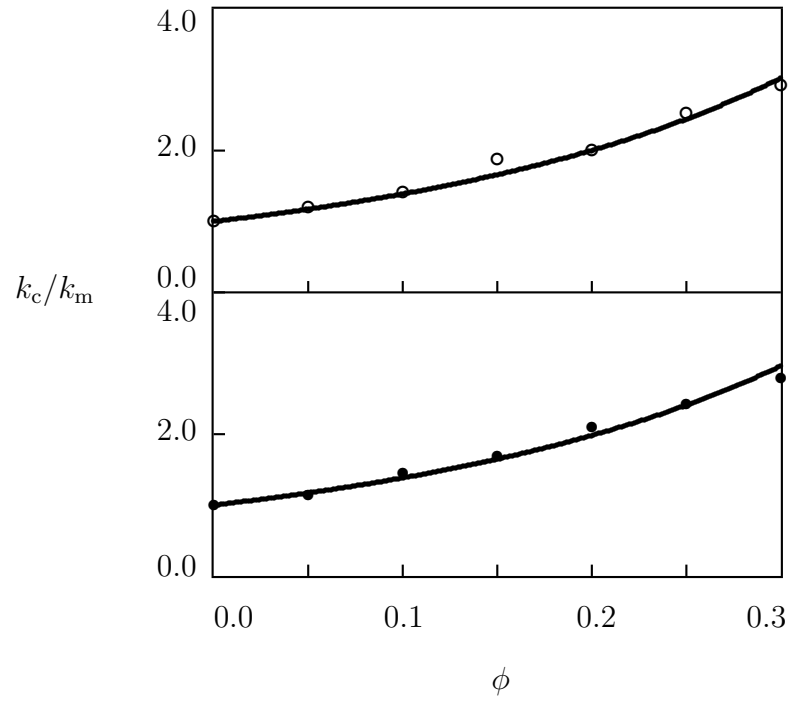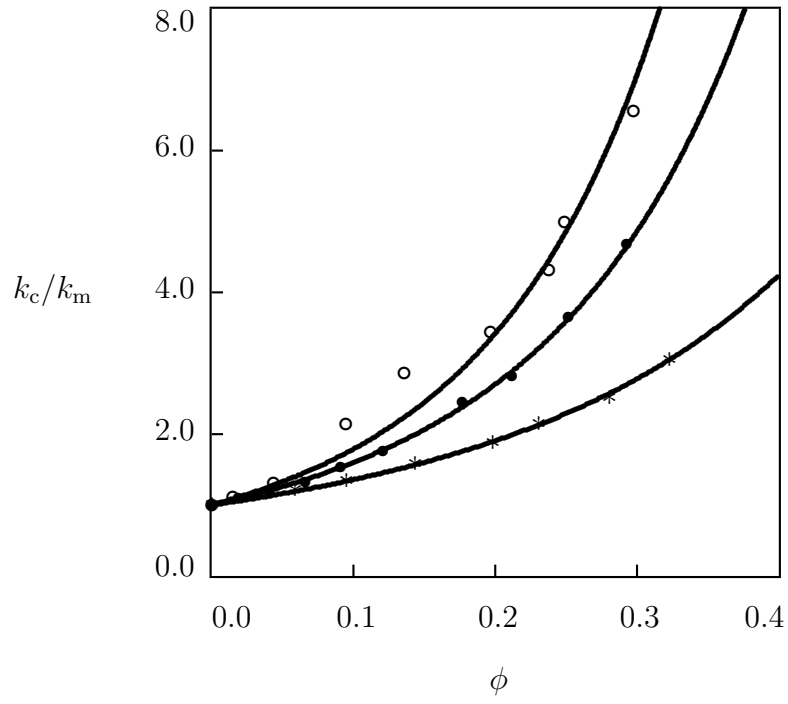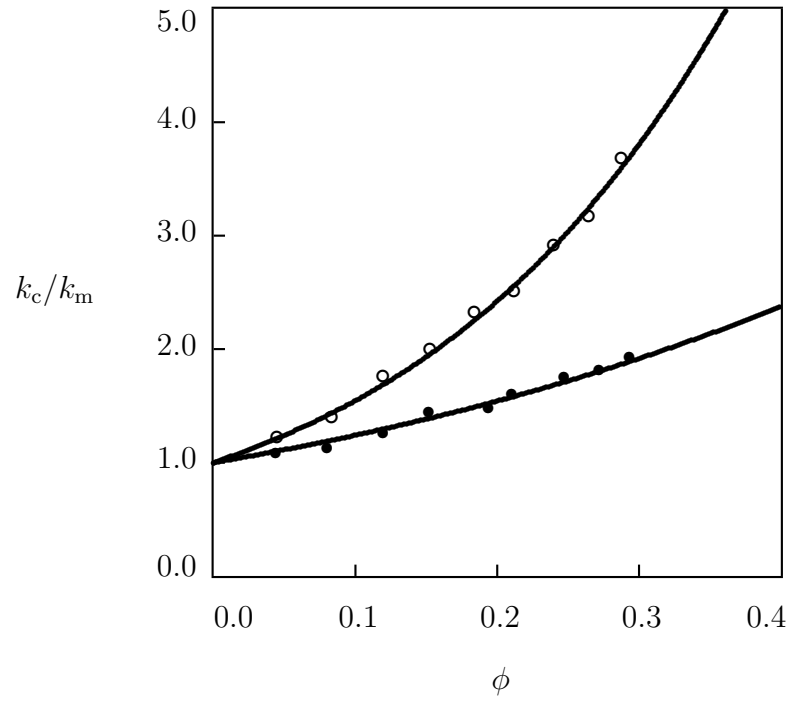
Figure 1:

Figure 2:

Figure 3:

Figure 4:

Figure 5: